ISSN: 0975-833X

Available online at http://www.journalcra.com

International Journal of Current Research
Vol. 11, Issue, 08, pp.6747-6760, August, 2019

DOI: https://doi.org/10.24941/ijcr.36453.08.2019

INTERNATIONAL JOURNAL OF CURRENT RESEARCH

RESEARCH ARTICLE

PALYNOLOGY, PALYNOFACIES AND MATURATION OF SEDIMENTS FROM MVULE # 1 WELL, TANZANIA

[1, 2, *]Mkuu, D.E., [1]Harding, I.C., [1]Marshall, J.E.A. and [2]Pearce, M.

[1]Ocean and Science, University of Southampton, National Oceanography Centre Southampton (NOCS), European Way, Southampton, SO14 3ZH, UK
[2]Tanzania Petroleum Development Corporation, Directorate of Upstream, P.O. Box 2774, Dar-Es-Salaam, Tanzania
[3]Evolution Applied Limited, Horseshoe Lodge, Horseshoe Lake, Little Farringdon, Gloucestershire, GL7 3QQ, UK

ARTICLE INFO

Article History:
Received 17th May, 2019
Received in revised form
25th June, 2019
Accepted 19th July, 2019
Published online 31st August, 2019

Key Words:
Tanzania,
TOC,
Palynofacies,
Palynomorphs,
Maturity,
Hydrocarbon generation

Corresponding author:* **Mkuu, D.E.

ABSTRACT

The Cretaceous strata of the Mvule # 1 well from the Deep Offshore Basin of Tanzania contain large amount of shale and laminated mudstone, which under favourable conditions may be possible potential source rocks for hydrocarbons. This study examines hundred samples from early to late Cretaceous age by means of total organic carbon (TOC) content, palynofacies analysis and thermal maturities. These analyses have been performed to determine the hydrocarbon source rock potential, kerogen type, maturity level of the source rocks and to provide the biostratigraphic framework of these Cretaceous sediments. The organic richness from Mvule # 1 well (TOC - all in wt %) ranges from 1.0% - 3.4%. Palynofacies particles represent mixed macerals with clear higher abundance of marine influenced and black wood materials inferring marine depositional environments under oxygen-deficient bottom water. Four palynofacies zones have been recognised and presented here. Palynomaceral components from Mvule # 1 well are characterised by kerogen type II and III respectively. Vitrinite reflectance measurements of this well range from 0.7% - 1.6% Rv indicating maturity levels that encompass the entire oil and gas window. Preservation of palynomorphs is relatively poor to well preserve. This paper presents fifty-two species recorded from a total of thirty cutting samples ranging from interval 3700m - 4800m with the exceptional samples (ranging from 4150 - 4800m) that yielded moderate to good preserved palynomorphs assemblages for identification. The studied sections of the Mvule # 1 well contain a distinct palynological association dominated by abundance species including *Classopollis classoides, Criboperidinium muderongense, Pterodinium cingulatum, Spiniferites twistringensis* and *Subtilisphera perlucida*. Common species such as *Exesipollenites tumulus, Sepispinula huguoniotii, Litosphaeridium siphoniphorum, Dinopterygium tuberculatum, Odontochitina operculatum,* and *Cyclonephelium sp.,* were also present, including rare species assemblages of *Adnatosphaeridium tutulosum, Hapocysta peridictya* and *Florentinia mantelii*.

***Citation: Mkuu, D.E., Harding, I.C., Marshall, J.E.A. and Pearce, M.*, 2019.** "Palynology, palynofacies and maturation of sediments from mvule # 1 well, Tanzania", *International Journal of Current Research*, 11, (08), 6747-6760

INTRODUCTION

The Mvule # 1 well was drilled in Block 5, offshore Tanzania by the Petrobras International Oil Company in 2010. Geographically, it is located at 07° 49′ 30″ and 40° 14′ 24″ in the Deep Offshore Basin in the Indian Ocean, and was drilled in a water depth of 600m (TPDC 2005; Fig. 1). The entire stratigraphic succession through which the well was drilled has previously been determined as Late to Early Cretaceous down to the base of the hole, a depth of 4832m (Fig. 2).

The Deep Offshore Basin of Tanzania is one of the country's most promising hydrocarbons provinces, and the site of several discoveries of natural gas. However, there is little published information regarding the biostratigraphy of Tanzanian sediments, source rock analysis, or thermal maturity studies. Alongside the and the Tanzania Petroleum Development Corporation, international exploration companies are undertaking exploration in the area with an aim of understanding the source rock accumulation, preservation of organic matter and hydrocarbon potential from the Deep Offshore Basin.

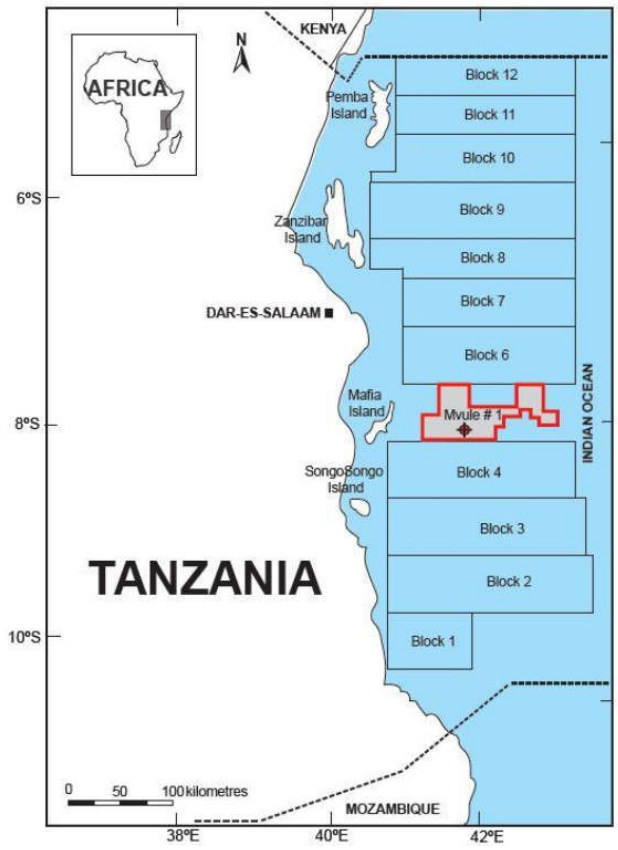

Fig. 1. Simplified map of Tanzania showing Block 5 in the Deep Offshore Basin, and the location of the Mvule # 1 well.

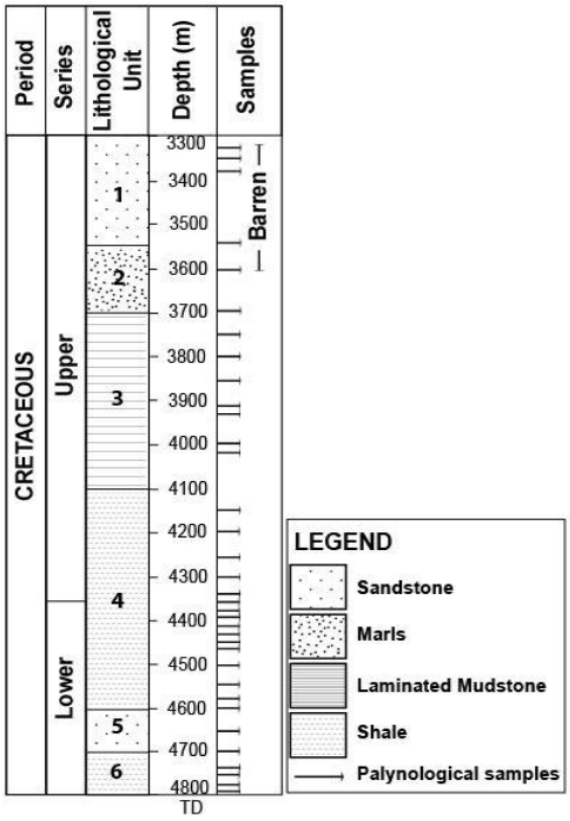

Fig. 2. Log showing lithostratigraphic succession in Mvule # 1 well with original age interpretation by TPDC, (2005)

This paper focuses on the Cretaceous sediments encountered in the offshore Mvule #1 well, particularly examining palynomorph distribution and biostratigraphy, organic matter composition (palynofacies analysis) and thermal maturity, in order to provide a biostratigraphic framework for future local and regional stratigraphic correlation and to identify potential source rocks for hydrocarbon generation. We establish a palynological bioevents for the Cretaceous of Tanzania, identify key species that may be useful for correlation purposes, using first downhole occurrences (FDOs) of palynomorph taxa. Comparisons are drawn with published studies from other Cretaceous palynofloral provinces covering regions of northern and western Africa, Australia and South America.

***Previous studies*:** The discovery of natural gas in the Deep Offshore Basin of Tanzania provided a major impetus for the hydrocarbon exploration in the area, although most of the scientific findings from these basins have not been published. However, there have been a limited number of publications on Tanzanian Cretaceous palynology, such as Mayagilo (1989), Balduzzi *et al*. (1992), Srivastava (1994), Srivastava and Msaky (1999), Schrank (1999, 2005, 2010) and more recently by Msaky (1995, 2000, 2007, 2008 and 2011), but many of these studies focus on palynostratigraphy of outcrop or cutting samples from onshore basins. Msaky (2011) established a biozonation based on mid Jurassic-earliest Cretaceous palynofloras from the coastal basins of Tanzania. There are very few published source rock studies from Tanzania, and all of these are based on onshore, rather than offshore material. For example, Kagya (1987) and Kagya *et al*. (1991) examined the source rocks and hydrocarbon potential (Permian age) from Nyasa Rift Basin, and oil shows from the southern part of the East African Rift Valley. Mpanju and Philp (1994) focussed on the bituminous sands (Early-Mid Jurassic) from Msimbati (Wingayongo) area and condensates from Tundaua (Mid Eocene) from Pemba Island, and Kagya (1996) characterised the geochemistry of Triassic source rocks from the Mandawa Basin; Mpanju *et al*. (1998) studied the hydrocarbon potential of Permian sediments in Tanzania, and finally, Semkiwa *et al*. (1998) investigated the geology, petrology and organic geochemistry of the Karoo (Late Carboniferous-Triassic) sediments from the Songwe-Kiwira coalfield.

Geological setting and Stratigraphy

Tectonic history and palaeogeography: Two major rifting phases are of importance in the development of the Deep Offshore Basin of Tanzania. First, the Karoo rifting phase (300-205 Ma) occurred from the late Carboniferous-Triassic periods; major rift structures were formed during this phase of tectonism and a broad depression was filled by thick terrigenous sequences (Salman and Abdula 1995). The second phase of rifting in the Mesozoic-Cenozoic (205-157 Ma), resulted from the break-up of Gondwana (TPDC 1979, Kajato 1989, Mbede 1991, Kapilima 2003). By the early Cretaceous, the breakup of the Gondwanan supercontinent had commenced with the south-to-north separation of South America and Africa to initiate the South Atlantic Ocean, and the progressive separation of the African and Madagascan-Indian continental blocks to open up the West Somali Basin (Kent *et al.* 1971, Watkins *et al*. 1992, Schluter and Hampton 1997). Around 95 Ma, a shallow shelf extended from the eastern margin of the 'South African' landmass, narrowing dramatically from north to south (towards the present day location of Tanzania), and descending offshore into the deeper waters of the West Somali Basin proper (Torsvik and Cocks 2017). From the late Cretaceous, around 90 Ma, major rifts developed within the African continent which divided Africa into five major tectonic

blocks (South Africa, North-East Africa, North-West Africa, Somalia and the Lake Victoria Block; Torsvik and Cocks 2017). During the early-mid Cretaceous Tanzania was located further south than today, lying at approximately 30°S (Figure 3; Torsvik and Cocks 2017).

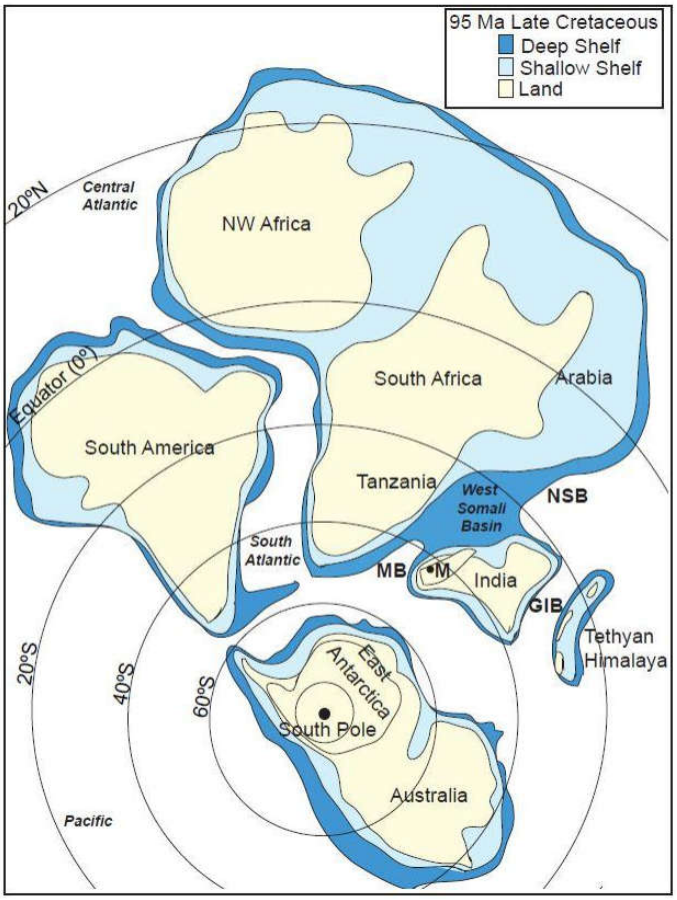

GIB-Greater India Basin; MB-Mozambique Basin; NSB-North Somali Basin; M-Madagascar

Fig. 3. Paleogeographical map during Late Cretaceous period (95 Ma) showing Gondwana fragmentation and position of Tanzania during Late Cretaceous (Torsvik & Cocks, 2017).

Palynofloral Provinces: From the Albian to Cenomanian the area to the north of present day Tanzania was characterised by palynomorphs representative of the Elaterates Province, whilst to the south lay the Austral Trisaccates Province (early Cretaceous-Cenomanian; Herngreen *et al*. 1996). Tanzania was located between these two floral provinces, in an area described as "Transitional" (Herngreen *et al*. 1996; Figure 4). Characteristic palyonological taxa of the mid Cretaceous Elaterate Province are found in strata extending as far as 30ºN and 30ºS, and include such distinctive taxa as *Afropollis, Schrankipollis* and *Pennipollis* spp. (which occur widely across Africa), and the Elaterate group of pollen (that are common in the Cenomanian of West African basins), both of which are commonly used as Albian-Cenomanian indicators from Western to Northeastern Africa (Jardine and Magloire 1965; Kaska 1989, Herngreen *et al*. 1996; Schrank 1990, 1994, 2001, 2005, 2010, 2017; Eisawi *et al*. 2012; Deaf *et al*. 2014; Atta-Peters, 2013; Atta-Peters *et al*. 2016; Cole *et al*. 2017). Indeed, species of these more northern elaterates have been sporadically recorded from the areas that were within the Transitional Province, such as Patagonia (Barreda and Archangelsky 2006; Archangelsky *et al*. 2009; Pramparo *et al.* 2016.), and even Tanzanian borehole material (Srivastava and Msaky 1999).

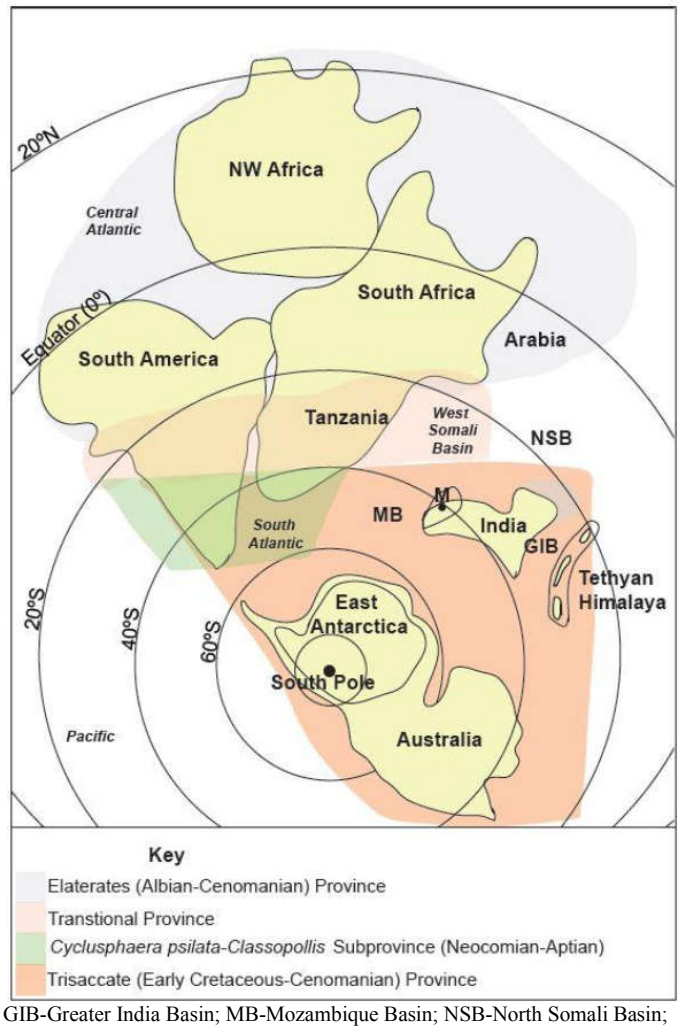

GIB-Greater India Basin; MB-Mozambique Basin; NSB-North Somali Basin; M-Madagascar

Fig. 4. Early Cretaceous-Cenomanian palynofloral provinces (Herngreen *et al.*, 1996), showing Tanzania palynoflora in transitional province

Conversely, assemblages from the Trisaccates Province may include such geographically widespread spore taxa as *Cicatricosisporites, Classopollis, Cycadopites, Podocarpidites, Ruffordiaspora,* which can be found in areas such as Western Australia, but demonstrate similarities to assemblages from the Kimmerdgian-Aptian successions of the Upper Tendaguru Beds of Tanzania (Schrank 2010).

Lithostratigraphy

The section of the Mvule # 1 well studied here penetrated a sedimentary succession believed to be of Cretaceous age (TPDC 2005). As there is no recognised lithostratigraphic nomenclature, the lithological unit are informally numbered, as shown in Figure 2, the boundaries between the lithostratigraphic units being defined by marked changes in lithology. Progressing in a top-down direction, the youngest lithostratigraphic unit, Unit 1, comprised of coarse grained and poorly sorted whitish sandstones, some 250m thick from a borehole depth of 3300 m to 3550 m. Below this lies Unit 2, from 3550 m - 3700m, characterised by greyish marls, fined grained, well sorted. Samples from both of these units were found to be palynologically poor or barren, and thus not included in this study. Samples below 3700 m proved to be more palynologically productive, and those from 4350 m to 4500 m were the most productive. Unit 3 is 400 m thick,

extending from 3700 m to a depth of 4100 m, and is comprised of dark grey laminated mudstones. Below this lies about 500m of grey shale, fine grained and well sorted (Unit 4). The underlying Unit 5 (4600 m - 4700 m) consists of whitish, medium to fine grained and moderately to well-sorted sandstone. Unit 6 is the deepest lithostratigraphic unit penetrated by the Mvule # 1 well, comprised of about 100 m thick of fine grained shale, from 4700 m - 4800 m (TD).

MATERIALS AND METHODS

A total of one hundred cutting samples obtained from the Mvule # 1 well have been analysed in this study, samples were collected at ten metre intervals.

Total organic carbon (TOC) analysis: Two subsamples from each sample were prepared for total organic carbon content (TOC weight %). Dried samples were crushed to powder and each split into two subsamples, one for total carbon (TC) analysis and the other for acidified carbon (AC - carbonate carbon removed) analysis. No further preparation of TC subsamples was required prior to analysis. To conduct the AC analyses, subsamples were first treated with 5-10 ml of Milli-Q water in glass test tubes, and then acidified by adding one to two drops of 37% hydrochloric acid to initiate decalcification. The sample solution was shaken slowly and carefully to avoid overly vigorous reactions, after which successive drops of hydrochloric acid were added until no further reaction was observed, then 10 ml of 37% hydrochloric acid was added and left overnight to ensure all carbonate dissolved. Mill-Q water was used to neutralise subsamples and they were then dried in an oven at low temperature. Five grammes of dry, powdered samples from each subsample (TC and AC) were sealed inside tin capsules for analysis using a Carlo Erba EA 1108 elemental analyser. The analyses were calibrated by conducting analyses of two standards of known carbon content after approximately every tenth subsample analysed; these were a low organic carbon sediment standard (LOSS - 1.5% TOC) and a high organic sediment standard (HOSS - 6.1%).

Palynofacies and palynomorph analyses: Between 5-10 g of each cutting sample were processed using standard palynological processing techniques (see Wood *et al*. 1996). First, concentrated 37% hydrochloric acid was added to remove carbonates, and then treated with concentrated 60% hydrofluoric acid to remove silicates. Each acidification step was followed by repeated washing of the samples to neutrality and sieving using a 15 µm nylon mesh. Sample residues were then boiled in concentrated 37% hydrochloric acid to remove neo-formed fluoride precipitates. Sample residues were then again neutralised using deionised water before the final sieving process, and stored in labelled plastic vials. Three drops of dispersant (detergent) were added to each aqueous residue before strew-mounting on a glass coverslip to achieve a reasonable palynomorph density and to minimise clumping, and left overnight to dry. The dried coverslips were mounted on labelled glass microscope slides using Elvacite 2044 mounting media. Examination of sedimentary organic matter (palynomacerals) and palynomorphs was made using an Olympus BH-2 transmitted light microscope. Identification and classification of palynomacerals followed those described by Bergen *et al.* (1990). Where possible, three hundred palynomaceral particles (phytoclasts, palynomorphs and amorphous organic matter [AOM] particles) were counted from each palynological sample to characterise the variability and assess changes in palynofacies composition. Form samples with low organic content, a minimum of one hundred particles were counted. A palynofacies zonation scheme was created using the Tilia© computer program by running a stratigraphically constrained CONISS cluster analysis of the palynomaceral percentage data, using square root transformations of data according to the Edwards and Cavalli-Sforza (1967) chord distance. Depositional environments of the each palynofacies zone were interpreted by using ternary AOM-phytoclasts-palynomorphs plots after Tyson (1993, 1995). A total of two hundred specimens of dinoflagellate cyst ('dinocysts') were identified per sample. Species range charts were created using the Stratabugs© program. First downhole occurrences (FDOs) and last downhole occurrences (LDOs) have enabled the identification of biostratigraphically important palynomorph taxa in this borehole. Photomicrographs were made using an Olympus BH-2 microscope fitted with an Olympus SC30 camera. Images of well-preserved specimens were processed using Analysis get IT image TWAIN program and illustrated in plates 1-3. The photomicrographs were taken using x40 objectives and plates were made by magnified photographs by approximately 500 times the original size unless otherwise indicated.

Vitrinite reflectance analysis: Twenty samples identified as being kerogen-rich were prepared for maturity studies. Slides for vitrinite measurements were made from palynological residues using the method of Hillier and Marshall (1992). Coverslips were sprayed with polishing thin film epoxy (PTFE) releasing agent before strewing the aqueous palynological residue on the coverslip and leaving it to dry. Dried cover slips were then mounted onto frosted glass slides using Fastglass resin, and left to harden. Coverslips were then removed carefully using a razor blade, leaving the resin-embedded kerogen particles exposed on the surface of the slide, before being ground down with 2500 grade emery paper. This was followed by the repeated polishing using successively finer alumina oxide powder (9.5, 3, and 0.5 µm) using a Kemet polishing pad on a Kemet Metkon Forcipol 300-IV grinder, using glycerine oil to fix the slides to the grinder holding plate. Finally, slides were rinsed using deionised water. Vitrinite particles in the prepared slides were then examined on a Zeiss UMSP-50 reflected white light microscope fitted with a x40 oil immersion objective. Two standards for reflectance were used in this study, dependent on the reflectivity level of the sample: the lower reflectivity YAG standard (yttrium aluminium garnet: 0.919%) and the higher reflectivity 3G standard (gadolinium germanium garnet: 1.727%). Where possible, reflectivity measurements were made of one hundred vitrinite particles from each sample, with a minimum of fifty measurements for samples which contained fewer such macerals.

Burial modelling: The burial histories of the investigated wells were modelled against the measured vitrinite reflectance data. An initial calibration of peak burial temperature, was determined from the mean random vitrinite reflectance *versus* measured burial heating temperature according to Barker and Pawlewicz (1994): in Mukhopadhyay and Dow (1994) as shown in Equation 1 below: -

Equation 1: $T = (\ln Rv + 1.68) / 0.0124$

Where T = maximum estimated burial temperature (°C)
lnRv = natural logarithm of vitrinite reflectance

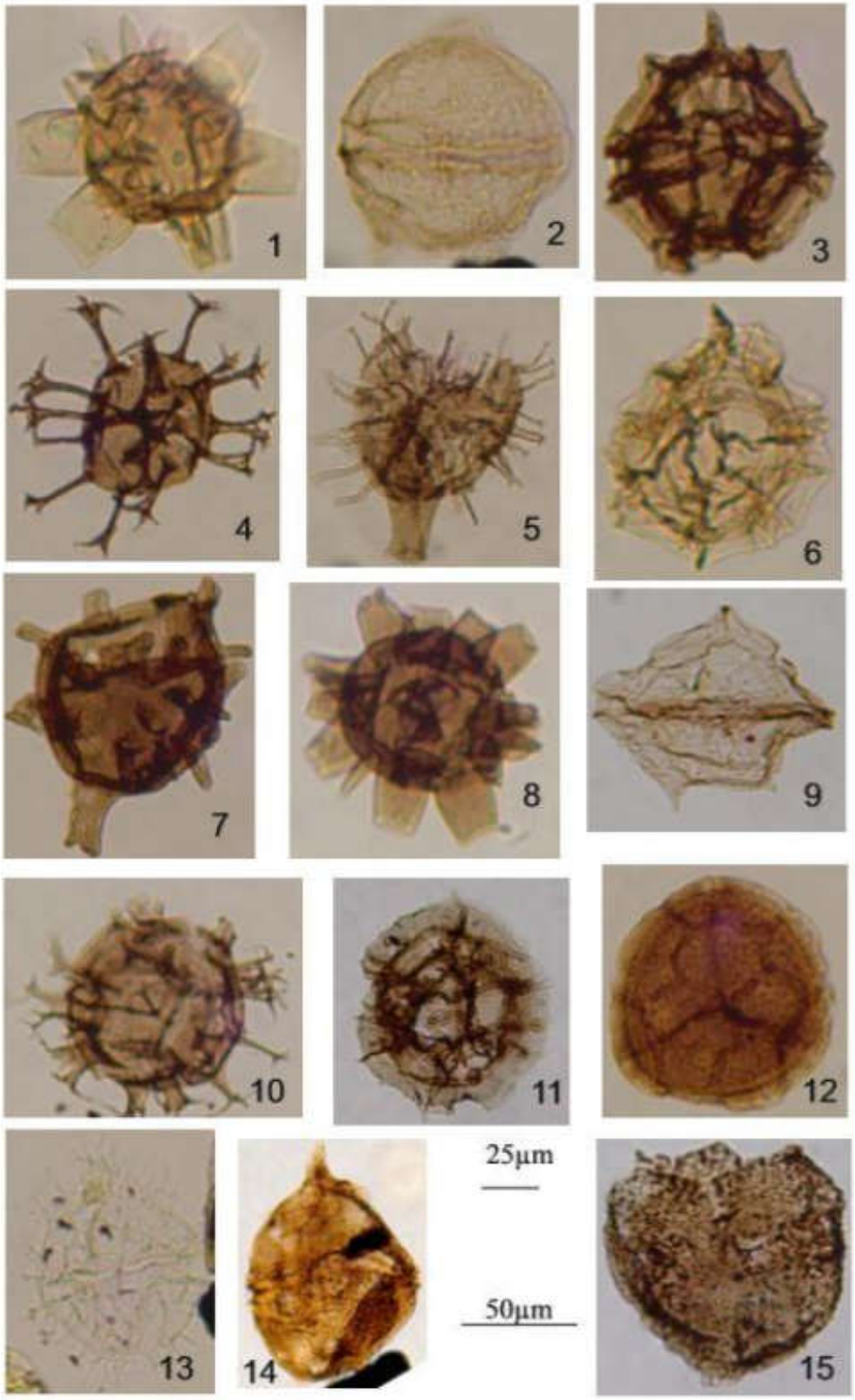

PLATE 1

Figs. 1 & 8: *Litosphaeridium siphoniophorum siphoniphorum*. Cookson & Eisenack,(1958)
Fig. 1: Mvule # 1, 4380 m, Slide 1, E.F. No. (L64/4), 10 µm
Fig. 8: Mvule # 1, 4410 m, Slide 1, E.F. No. (K66/1), 67 µm
Figs. 2: *Subtilisphaera Perlucida.* (Alberti) Jain & Millepied (1973) Mvule # 1, 4380 m, Slide 1, E.F. No. (S44/3), 39 µm
Figs. 3: *Pterodinium Cornutum*. Wetzel (1933b) Mvule # 1, 4430 m, Slide 1, E.F. No. (E55/3), 63 µm
Figs. 4: *Oligosphaeridium asterigerum*. Gocht (19590 Mvule # 1, 4200 m, Slide 1, E.F. No. (N59/2), 39 µm
Figs. 5: *Florentinia mantelii,* (Davey & William) Davey & Verdier (1973) Mvule # 1, 4430 m, Slide 1, E.F. No. (K67/1), 63 µm
Figs. 6: *Pterodinium Cornutum*. Cookson and Eisenack (1962b) Mvule # 1, 4380 m, Slide 1, E.F. No. (E54/3), 60 µm
Figs. 7: *Florentinia sp.* (Davey & Williams) Davey & Verdie (1973) Mvule # 1, 4430 m, Slide 1, E.F. No. (K60/2), 45 µm
Figs. 9: *Palaeoperidinium cretaceum*. Pocock (1962) Mvule # 1, 4150 m, Slide 1, E.F. No. (L60/2), 45 µm
Fig. 10: *Spiniferites ramosus*. (Ehrenberg) Loeblich & Loeblich (1966) Mvule # 1, 4380 m, Slide 2, E.F. No. (V40/2), 38 µm
Figs. 11: *Dinopterygium tuberculatum*. Stover and Evitt (1978) Mvule # 1, 4380 m, Slide 1, E.F. No. (E48/3), 50 µm
Fig. 12: *Rouseisporites reticulates*. Pocock (1962) Mvule # 1, 4380 m, Slide 1, E.F. No. (O50/2), 15 µm
Fig. 13: *Paleohystrichophora infusoiriodes.* Cookson and Eisenack (1970a) Mvule # 1, 4380 m, Slide 1, E.F. No. (D51/3), 62 µm
Figs. 14: *Criboperdinium muderongense*. Cookson and Eisenack (1958) Mvule # 1, 4430 m, Slide 1, E.F. No. (O64/4), 5 µm
Fig. 15: *Cyclonephelium* sp. Deflandre and Cookson (1955) Mvule # 1, 4200 m, Slide 1, E.F. No. (E54/3), 67 µm

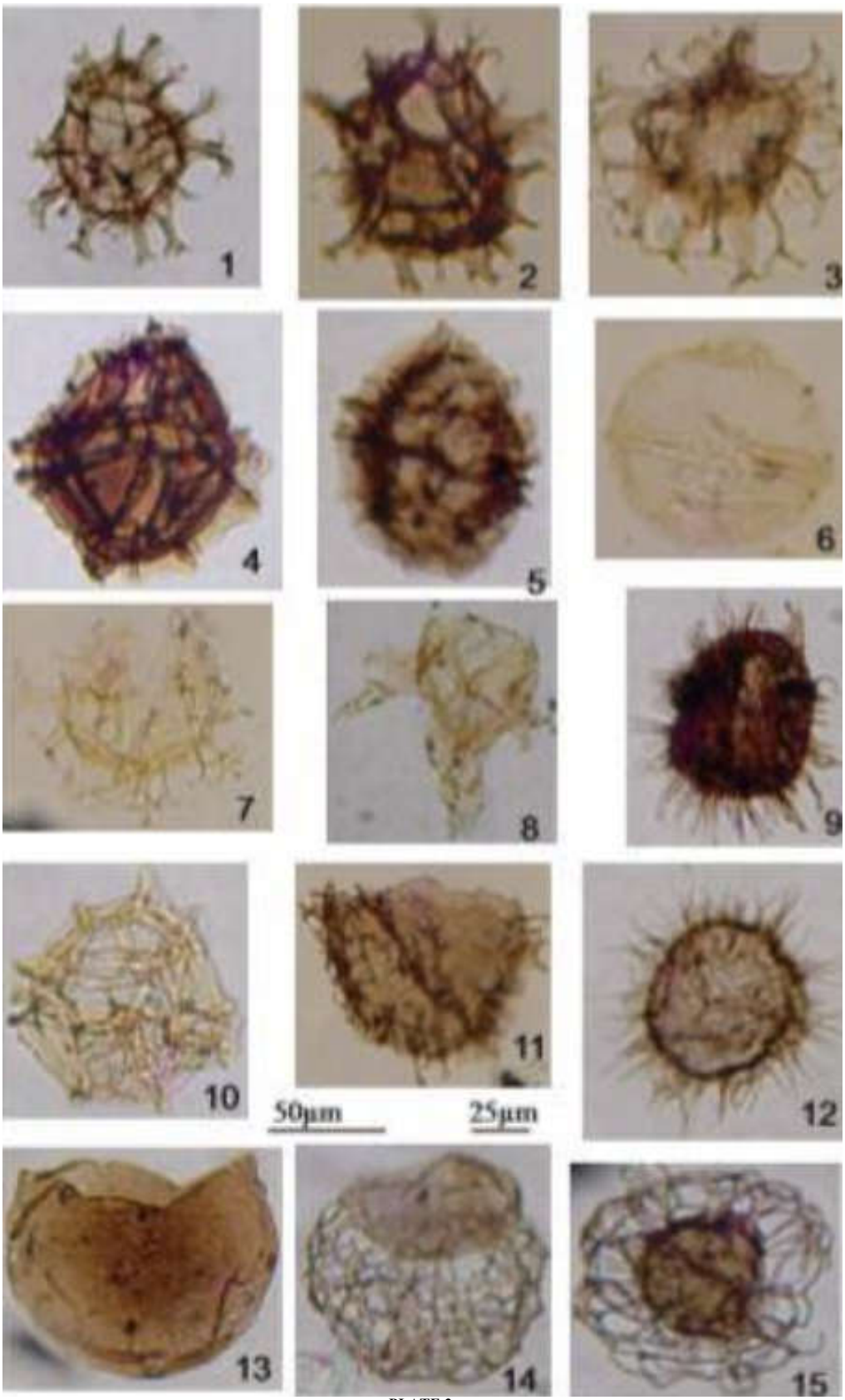

PLATE 2

Fig. 1-3: *Spiniferites* sp. (Ehrenberg) Loeblich & Loeblich (1966); Mvule # 1, 4410 m, Slide 1, E.F. No. (E54/3), 67 µm; Mvule # 1, 4430 m, Slide 2, E.F. No. (F47/4), 45 µm; Mvule # 1, 4360 m, Slide 2, E.F. No. (V47/1), 51 µm

Figs. 4-5: *Pterodinium Cornutum*. Cookson and Eisenack (1962b); Mvule # 1, 4390 m, Slide 1, E.F. No. (E54/3), 67 µm; Mvule # 1, 4370 m, Slide 1, E.F. No. (N52/3), 55 µm

Figs. 6: *Subtilisphaera Perlucida.* (Alberti) Jain & Millepied (1973); Mvule # 1, 4450 m, Slide 1, E.F. No. (V40/2), 38 µm

Fig. 7: *Spiniferites twistringensis*. (Ehrenberg) Loeblich & Loeblich (1966); Mvule # 1, 3930 m, Slide 2, E.F. No. (D47/1), 51 µm

Fig. 8: *Xenascus ceratiodies.* Deflandre (1937b); Mvule # 1, 3920 m, Slide 1, E.F. No. (L55/2), 62 µm

Fig. 9: *Cometodinium sp.* Deflandre and Courteville (1939); Mvule # 1, 4390 m, Slide 2, E.F. No. (J46/1), 10 µm

Fig. 10: *Pterodinium Cornutum*. Cookson and Eisenack (1962b); Mvule # 1, 4390 m, Slide 1, E.F. No. (S35/3), 45 µm

Fig. 11: A*reoligera sp.* Lejeune-Carpentier (1938a); Mvule # 1, 4430 m, Slide 1, E.F. No. (V52/4), 8 µm

Fig. 12: *Cometodinium sp.* Deflandre and Courteville (1939); Mvule # 1, 4360 m, Slide 2, E.F. No. (L47/1), 55 µm

Fig. 13: *Sentusidinium explanatum.* Sarjeant and Stover (1978); Mvule # 1, 4390 m, Slide 1, E.F. No. (F47/2), 50 µm

Figs. 14-15: *Adnatosphaeridium tutulosum.* Cookson and Eisenack (1960a); Fig. 14: Mvule # 1, 4430 m, Slide 1, E.F. No. (J45/4), 8 µm; Fig. 15: Mvule # 1, 4450 m, Slide 1, E.F. No. (P69/1), 10 µm

PLATE 3

Fig. 1: *Cicatricosisporites australis* Cookson, 1953) Potonié (1956); Mvule # 1, 4200 m, Slide 1, E.F. No. (E47/2), 10 µm
Fig. 2: *Exesipollenites tumulus*. Balme (1957); Mvule # 1, 1, 4250 m, Slide 1, E.F. No. (L57/2), 5 µm
Figs. 3: *Chomotriletes minor. (*Kedves) Pocock (1970); Mvule # 1, 4150 m, Slide 2, E.F. No. (E62/3), 5 µm
Fig. 4: *Lycopodicarpites reticulates;* Mvule 1, 4200 m, Slide 1, E.F. No. (L56/3), 40 µm
Fig. 5: *Cicatricosisporites hughesii*. (Ehrenberg) Loeblich & Loeblich (1966); Mvule # 1, 4200 m, Slide 1, E.F. No. (T51/3), 60 µm
Fig. 6: *Laevigatosporites sp.;* Mvule # 1, 4380, Slide 1, E.F. No. (G64/4), 50 µm
Fig. 7: *Trileteporotes sp.;* Mvule # 1, 4200 m, Slide 2, E.F. No. (F47/4), 45 µm
Fig. 8: *Ruffordiaspora australis*.; Mvule # 1, 3920 m, Slide 1, E.F. No. (P66/4), 9 µm
Fig. 9: *Concavisporites sp.;* Mvule # 1, m, Slide 1, E.F. No. (K52/3), 80 µm
Fig. 10: *Exesipollenites tumulus.* Balme (1957); Mvule # 1, 4380 m, Slide 2, E.F. No. (J65/4), 51 µm
Fig. 11: *Odontochitina costata*. Alberti (1961); Mvule # 1, 1, 4150 m, Slide 1, E.F. No. (K67/2), 80 µm
Fig. 12: *Ephedripites striatus.* Balme & Hennelly Potonié (1958); Mvule # 1, 44150 m, Slide 2, E.F. No. (T42/1), 7 µm
Fig. 13: *Bisaccate sp.* Wilson & Webster (1946) emend Krutzsch,; Mvule # 1, 4410 m, Slide 1, E.F. No. (E63/2), 6 µm

This equation produces a peak temperature estimate from vitrinite reflectance that is used to start the burial modelling. Data in an Excel spreadsheet containing well top, thicknesses, formation units, age and lithologies were then input into *Genesis*© 15.4 software to construct burial history, thermal history, and hydrocarbon generation of the well. A burial graph profile from *Genesis* was then modelled to produce calculated vitrinite reflectance from the well, to compare with measured data, to assess the veracity and robustness of the model's subsidence modelling and formations that entered hydrocarbon generation. Thermal parameters such as heat flow, geothermal gradients, water depth and past surface temperature during the Cretaceous - Paleogene from bivalve isotopic analyses (Pearson *et al*. 2007) have been used to build the model of the studied well.

RESULTS AND DISCUSSION

TOC Results: Results of the TOC analyses are presented in Figure 5, and the numerical data are presented in Table 1. TOC values range from the 1.0 - 3.4 %, and thus all samples analysed fulfil Jarvie's (1991) definition of potential source rocks: being those sediments with TOC levels above 0.5%. The upper part of laminated mudstone Unit 3, from 3700 m - 3800 m, has the lowest TOC contents in the well, ranging from 1.0 - 1.3%, whereas the lower part of this unit yielded TOC values varying from 1.7 - 2.6% (3850 m - 4050 m). Below this, the thick shale succession from 4100 m - 4550 m (Unit 4), showed the TOC values between 2.2 - 3.4%, the highest values in the entire well, but these drop with the lithological change at 4700 m into the sandstones of Unit 5, with TOC values of 1.8-1.9% between 4650 m - 4700 m. The deepest part of the studied section from 4700 m - 4800 m, the shales of Unit 6, have high TOC values, reaching 3.1% at 4800 m.

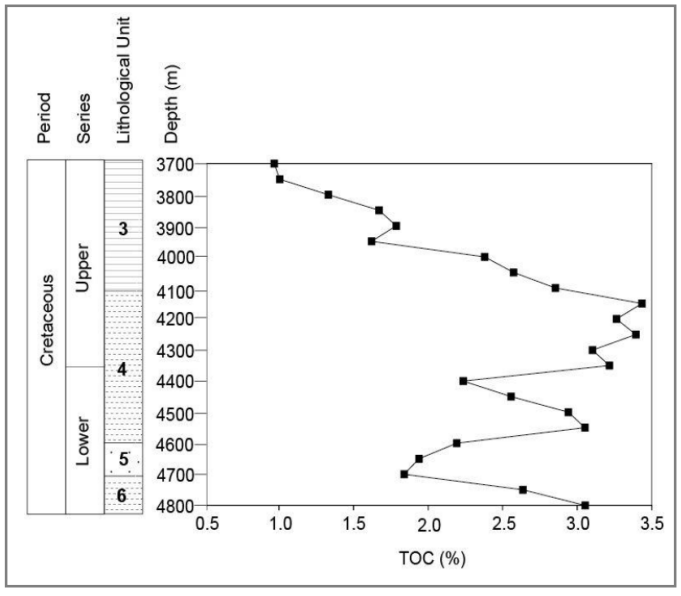

Fig. 5. TOC values for the Mvule # 1 well

Palynofacies Results: The relative abundances (%) of palynomacerals throughout the succession are shown in Figure 6, and the numerical data detailing the average palynomaceral compositions of each palynofacies zone identified through CONISS analysis are presented in Table 2. The palynomaceral relative abundance data has also been used to construct an APP ternary kerogen plot after Tyson (1993, 1995), in order to interpret environments of deposition (Figure 7).

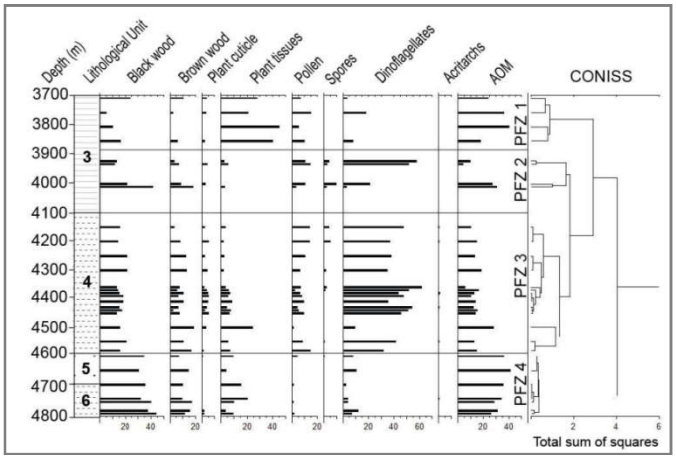

Fig. 6. Palynomaceral relative abundances, and the palynofacies zones defined by CONISS clusters inthe Mvule # 1 well

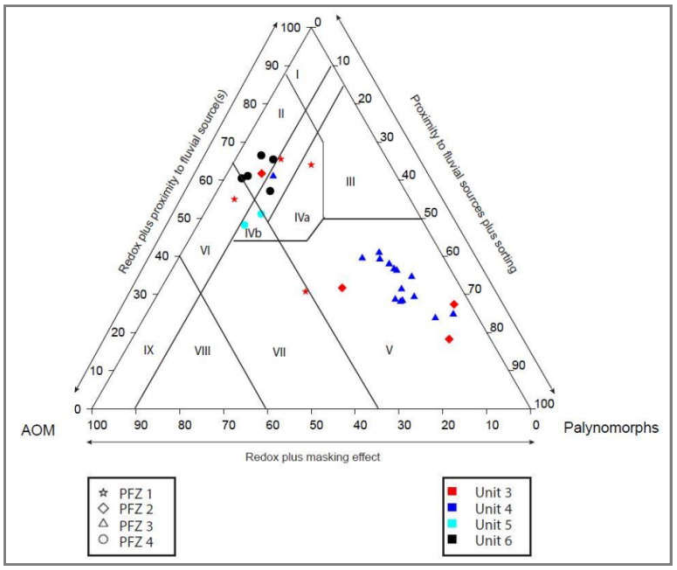

Fig. 7. Ternary AOM-phytoclasts-palynomorphs (APP) plot for the palynomaceral relative abundances of samples from the Mvule # 1 well after Tyson (1993, 1995). The symbols represent the palynofacies zone in which the sample is located, and the colour of that symbol indicates the lithological unit from which the sample comes.

Overall, samples from Mvule # 1 are dominated by high abundances of dinoflagellate cysts, phytoclasts and AOM; sporomorphs are of relatively low abundance throughout the succession. The presence of dinocysts in every sample confirms a marine depositional influence throughout the succession. Stratigraphically constrained CONISS cluster analysis of the palynomaceral percentage count data in Tilia has been used to define palynofacies associations. Samples from the upper part of the studied section from 3700 m - 3850 m of the laminated mudstone of Unit 3 fall into Palynofacies Zone 1 (PFZ 1), characterised by an average of 54% phytoclasts (mainly plant tissues rather than wood), 30% AOM and 17% palynomorphs (mainly pollen). This zone is dominated by terrestrially derived palynomacerals with low abundances of marine palynomorphs, indicating a much more proximal environment of deposition. More specifically, samples from PFZ 1 plot into field II in the APP ternary plot (Figure 7), indicating marginal dysoxic-anoxic shelf conditions during deposition. Palynofacies Zone 2 (PFZ 2) encompasses samples from 3920 m - 4010 m covering the middle to lower part of the laminated mudstone Unit 4, with average

palynomaceral contents of 48% palynomorphs (mainly dinocysts), 35% phytoclasts and 18% AOM. The samples from PFZ 2 fall in field V of the APP plot (Figure 7), indicating a more oxic offshore, mud-dominated distal shelf setting. Only one sample falls outside field V that at 4010 m, plotting in field II, indicating a brief return to the conditions prevailing during deposition of the younger sediments in PFZ 1. Palynofacies Zone 3 (PFZ 3) spans the thick shale Unit 4, including samples from 4150 m - 4580 m, which are dominated by averages of 51% palynomorphs (mainly dinocysts), and with slightly lower averages of phytoclasts (35%) and AOM (14%). Again, most samples from PFZ 3 plot in field V of the APP diagram (Figure 7) demonstrating the same oxic, offshore, mud-dominated distal shelf setting seen in PFZ 2. Only one sample falls outside field V, that at 4500 m plotting in field II, indicating a brief return to the conditions prevalent in PFZ 1. Palynofacies Zone 4 (PFZ 4) is restricted to the deepest part of the well from 4600 m to the base of the well 4800 m, this zone spans the entirety of the sandstones of Unit 5 and the deepest shales of Unit 6. Samples are characterised by average 59% phytoclasts, and high abundances of 33% of AOM, and lower abundances of palynomorphs, around 8% (mainly composed of dinocysts). The two samples from the sands of Unit 5 (4600 m - 4650m) are accounted as shale interbeds as they plot in field IVb of the APP diagram (Figure 7), demonstrating suboxic-anoxic depositional conditions, consistent with the coarser-grained lithology of the unit, whereas most samples from Unit 6 plot in field II of the ternary plot (Figure 7), indicative of marginal dysoxic - anoxic depositional conditions, save for one sample (4700 m) which plots in field VI, indicating more proximal suboxic-anoxic on the shelf at the time of deposition.

Palynological Results: A total of 52 marine and terrestrial palynomorph species were recorded in the studied interval between 3700 m - 4800 m, but species richness is extremely low throughout, averaging ~9 dinocyst species per sample and only ~2 sporomorph species. Indeed, the species richness in Mvule # 1 is highly variable, but is highest in the middle part of the borehole where marine richness reaches a maximum of 26 dinocyst species per sample and 6 sporomorph species. The paucity of recovered palynomorphs has proven problematic, as there are very few age-diagnostic taxa. Despite this issue, the majority of the assemblages contain typical Cretaceous sporomorphs such as *Classopollis classoides,* with several samples also yielding *Ephedripites striatus, Exesipollenites tumulus and Deltoidospora toralis*; the most abundant dinoflagellate cyst are *Pterodinium cornutum, Sentusidinium explanatum, Subtilisphera perlucida* and also the long-ranging *Spiniferites twistringensis,* with frequently encountered Cretaceous forms such as *Criboperidinium muderongese, Hystrichodinium pulchrum, Odontochitina costata, Oligosphaeridium asterigerum and Palaeoperidinium cretaceum*. However, despite the discovery in borehole material from the Tanzanian Coastal basins by Srivastava and Msaky (1999) of characteristic and age-diagnostic elaterate pollen taxa such as *Elaterosporites klaszii, E. protensus, E. verrucatus* and *E.* cf. *castelaini*, Elaterate Province sporomorphs are entirely absent from the Mvule # 1 samples. The absence of these key biostratigaphic indices in Mvule #1 may be due to taphonomic factors, such as winnowing (Mvule # 1 is located in a more offshore situation than the boreholes studied by Srivastava and Mskay, 1999), syn- or post-depositional oxidation, etc., or due to more localised ecological exclusion of taxa that were probably at the most southerly limit of their climatic tolerances (Cole *et al*. 2017). Furthermore, whilst 'absence' cannot be taken as proof of age, the lack of such pollen taxa as *Afropollis* and allied forms, and key dinocyst species such as *Aptea* and *Pseudoceratium*, suggests that sediments of Aptian age were not reached during the drilling of Mvule #1. The numerical abundances of the species identified are shown in Table 3, and their ranges organised by first downhole occurrence and also by last downhole occurrences (Figures 8). However, given the impoverished nature of the Mvule #1 palynological assemblages it is not possible to erect a formal biozonation scheme, so here we try to bracket the ages of the sediments penetrated in the well by identifying three dinocyst bioevents (1-3). Where possible we use first downhole occurrences (FDOs), although the relatively restricted number of often long-ranging taxa present has also required the use of last downhole occurrences (LDOs) to delineate these bioevents (Figure 9 and 10). The age assignments of the bioevents are established by comparing the biostratigraphic ranges recorded from other African, South American and Australasian localities, including the work of Srivastava (1976, 1978, 1981), Morgan (1975, 1977a), Burger (1980), Salami (1981), Uwins and Batten (1988), Helby *et al.* (1987). Schrank (1987, 1990), Kaska (1989), Schrank and Awadh (1990), Schrank and Mahmoud (1998), Schrank (2001), Eisawi and Schrank (2008, 2009), Deaf (2009), Eisawi *et al*. (2012), Chiaghanam *et al*. (2012), Deaf *et al*. (2014), Atta-Peters *et al*. (2015) and Cole *et al*. (2017).

***Biostratigraphy*:**

Bioevent 1: First downhole occurrence of *Litospheridium siphoniphorum* (Late Cenomanian)

The first downhole occurrence (FDO) of *Litosphaeridium siphoniphorum* (Unit 4 at 4150 m) is a diagnostic marker for the Late Cenomanian. The dating of the FDO of this species to the Late Cenomanian is supported by previous studies such as Dodsworth (2004) from Poland, Partridge and Dettmann (2003) and Partridge (2006) from Australia. Dodsworth (2000) and Pearce *et al*. (2009) documented the top consistent appearance and steady occurrence of *L. siphoniphorum* in the Late Cenomanian of southern England. Palynological assemblages from strata lying above this bioevent horizon are of very low species richness and lack age-diagnostic taxa, and thus these sediments can only be assigned a post-Cenomanian late Cretaceous age.

Bioevent 2: First downhole occurrences of *Adnatospheridium tutulosum* and *Hapsocysta peridictya* (intra-Late Cenomanian)

The FDOs of *Adnatospheridium tutulosum* and *Hapsocysta peridictya* in Unit 4 at 4390 m, are intra-Late Cenomanian events. In particular, the intra-Late Cenomanian FDO of *A. tutulosum* is supported by studies from England (Dodsworth 2004), the USA (Dodworth 2000, 2016), the Czech Republic (Skupien *et al*. 2003), Ukrain (Dodsworth 2004), England (Pearce *et al*. 2009) and New Zealand (Schiqler and Crampton 2014). The FDOs of *H. peridictya* is also supported by the work of Dodsworth (2004) from England and study from New Zealand by Schiqler and Crampton (2014).

Bioevent 3: Last downhole occurrences of *Palaeohystrichophora infusorioides* and *Adnatospheridium tutulosum* (Late Albian)

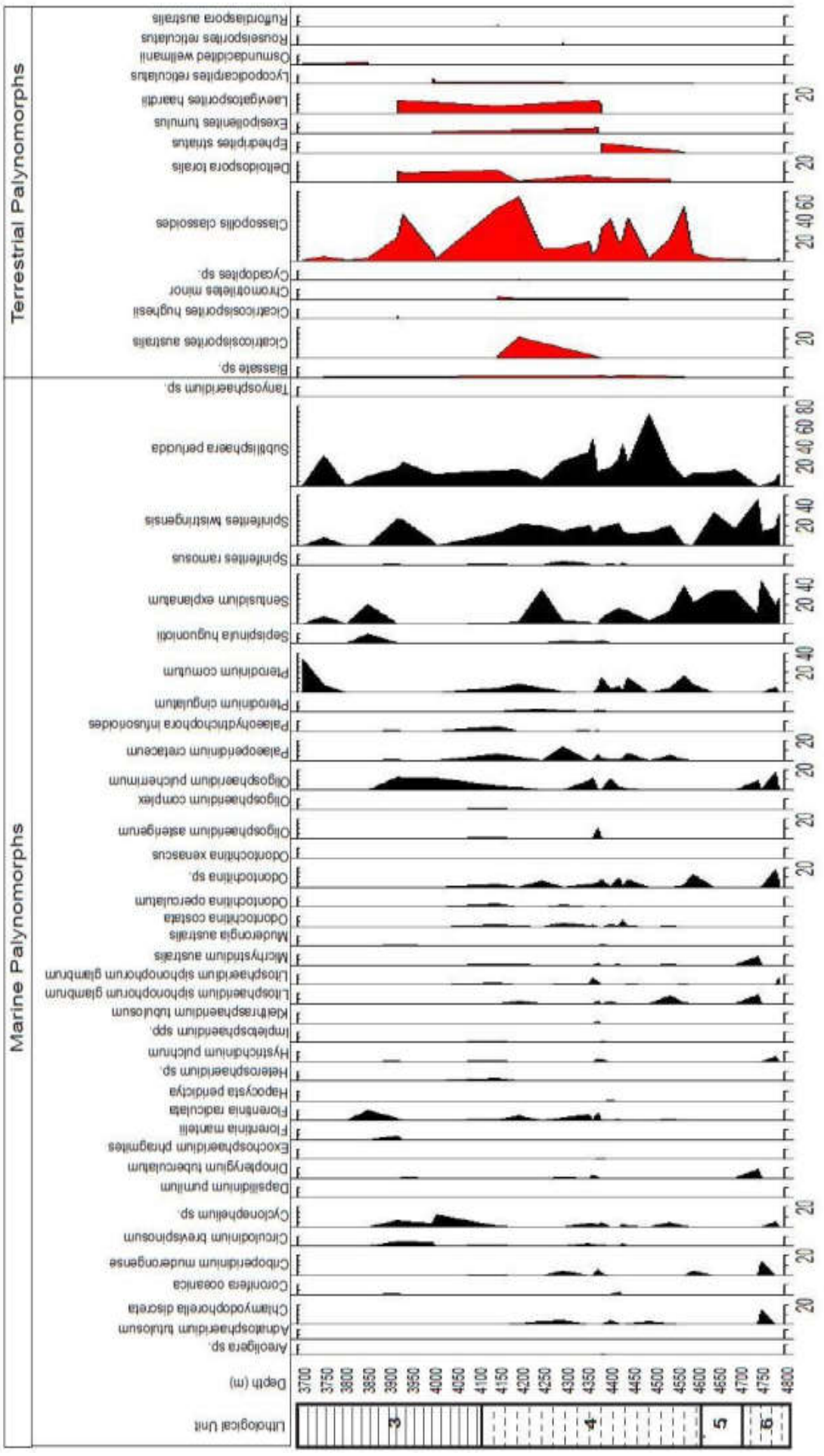

Fig. 8. Distribution chart of species found from the Mvule # 1 well

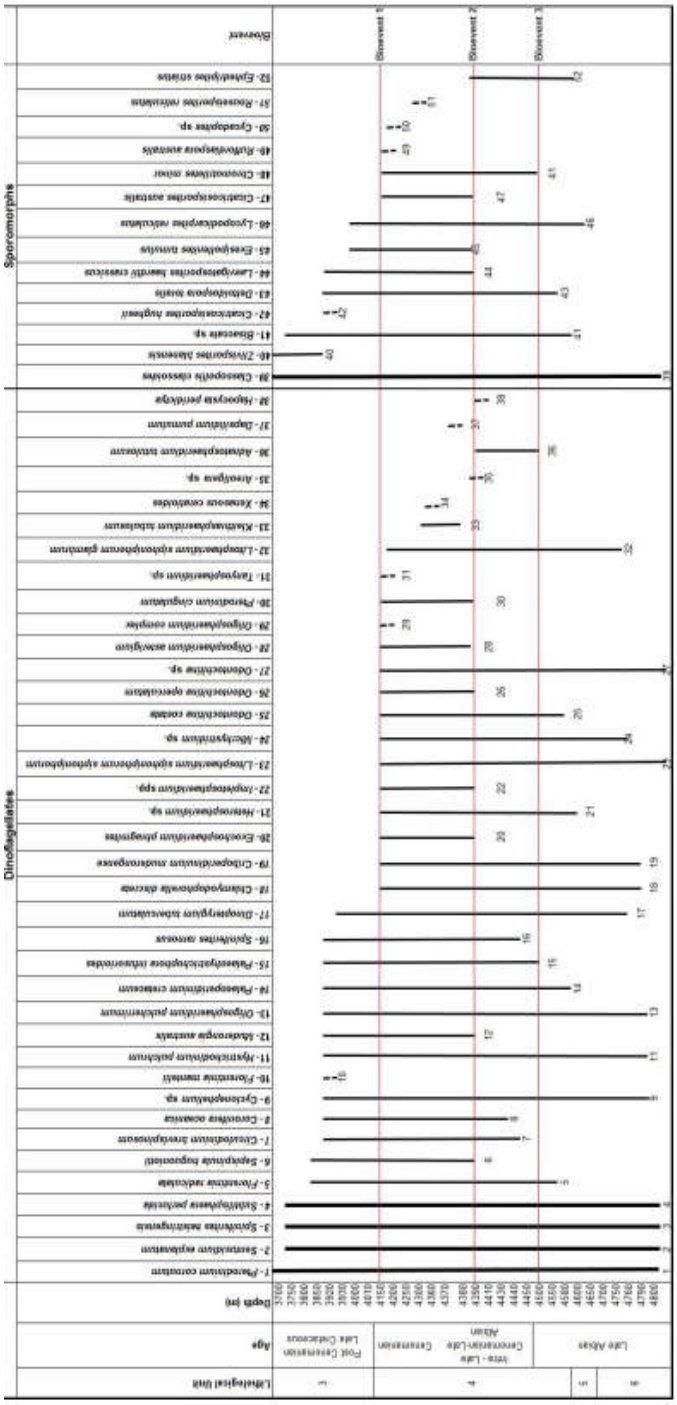

Fig. 9. Range chart for selected species showing biozones from FDO's of the Mvule # 1 well

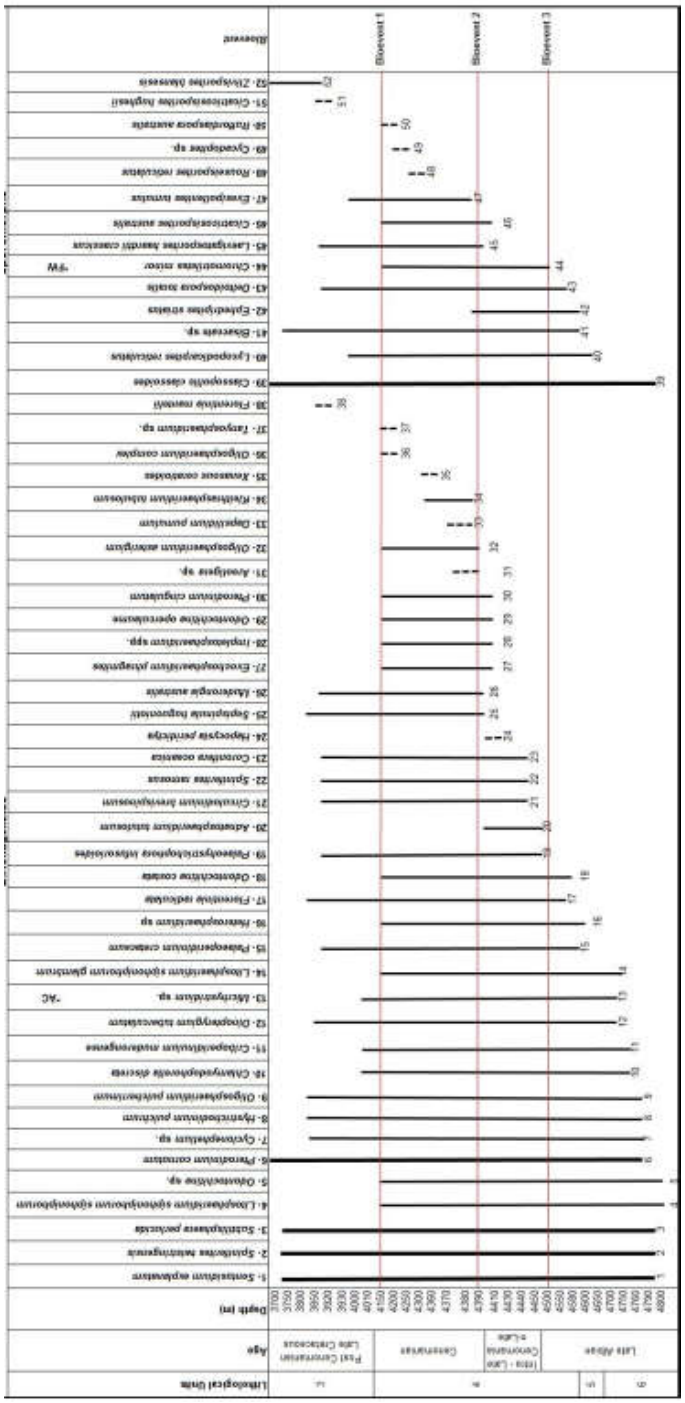

Fig. 10. Range chart for selected species showing biozones from LDO's of the Mvule # 1 well

The LDO of *Palaeohystrichophora infusorioides* at 4500 m (Unit 4) is a late Albian marker. This species has been reported to have an FDO in the late Albian in Libya (Uwins and Batten 1988), Morocco (Gubeli *et al*. 1984), Western Australia (Backhouse 2006), North African (Oboh *et al*. 2007), and the USA (Skupien *et al* 2009). Samples below Bioevent 3 contain a number of long ranging species in the late Albian but there no FOs recognised in the base of late Albian (Shale member Unit 6).

Thermal Maturity Results: A total of thirty vitrinite-rich samples were selected for thermal maturity analysis from the Mvule # 1 well, with a representative coverage of each lithological unit. Thermal maturity numerical data are shown in Table 4. Vitrinite reflectances (Rv) increase with burial depth as would be expected, with minor contamination by caving.

Reflectivity ranges from 0.7% to 1.6% Rv. The maturity levels are shown in Figure 11, the definition of the maturity zones follows the works of Tissot and Welte (1978). Samples from units 1 and 2, ranging from 3330 m - 3650 m, have entered the window for early liquid hydrocarbon generation, with reflectivity values range from 0.7 - 0.9% Rv. Below this, the laminated mudstone of Unit 3 (from 3700 m - 3800 m) are within the liquid hydrocarbon window, with reflectivity ranging from 1.0 - 1.3% Rv. One sample (3700 m) showed high reflectivity value of 1.3% Rv than it should not be expected in this unit, suggesting a reworked but after repetitive examination of vitrinite macerals, this sample was represented by more semi-fusinite material than vitrinite. The greyish shales of Unit 4 (4100 m - 4520 m) have reflectivity varying from 0.7-1.6% Rv (liquid hydrocarbon to dry gas zone). Caving samples have been noted at 4200 m and 4410 m where

reflectivity drops rather than increasing reflectivity in higher depths as it was expected.

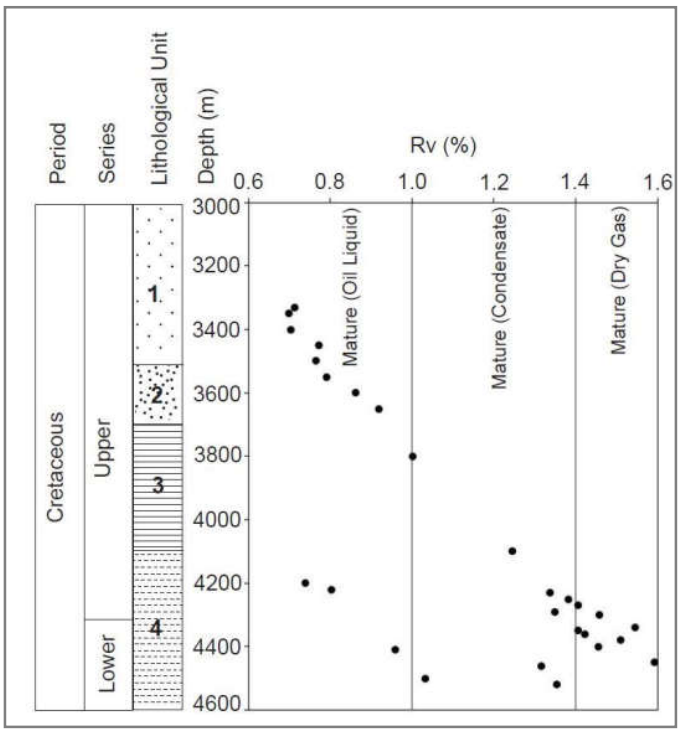

Fig. 11. Distribution of vitrinite reflectance values versus depth showing maturity zones of the Mvule # 1 well

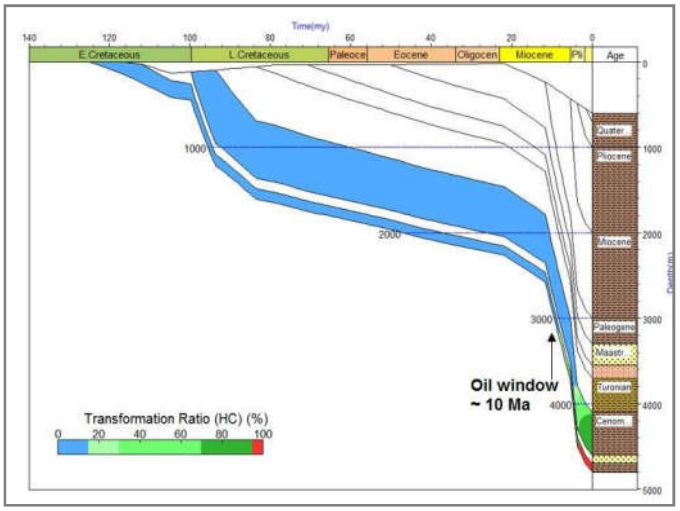

Fig. 12. Burial Model of the Mvule # 1 well

Burial Model: Burial model for the study well was created using *Genesis* software, and the results are shown in Figures 12. Maturation history in terms of burial and thermal evaluation was calibrated using measured vitrinite reflectance. The present day and palaeo-surface temperatures and water depths used to build the model of the studied wells are adopted from Pearson *et al*. (2007). Calibration of peak burial heat flow, reflecting maximum temperatures during burial of the study well, have been determined from the mean random vitrinite reflectance and just an approximation of estimated burial heating temperature from Barker and Pawlewicz (1994). The thermal gradient for the investigated well have been determined by using geothermometry calculations and plotted on the graph of vitrinite reflectance against depth. Geothemometry gradient have been calculated using Equation 1 (below) from Barker and Pawlewicz (1994) and used to produce an estimate to the start modelling:

Equation 1: $T = (\ln Rv + 1.68) / 0.0124$

Where T = maximum estimated burial temperature (°C)
lnRv = natural logarithm of vitrinite reflectance

In this regard, for Mvule # 1, mean random vitrinite reflectance, %Rv, is 0.7 to 1.5% from 3330 m – 4400 m. Estimated burial peak equivalent for these mean vitrinite reflectances range from 107° C to 169° C (Barker and Pawlewicz 1994). Therefore, 1 km for borehole depth over which these values occur is calculated as 4400 - 3330/1000 = 1.07 m. Burial peak difference = (T_{peak1} - T_{peak2}) = 169°C - 107°C = 62° C. Therefore, for 1 km the thermal gradient can be calculated as 62° C /1.07 m = 57.9° C/km ~ 58° C/km. The geothermal gradient of 58° C/km for Mvule # 1 reveal the thick sediment in the Shale Unit (~ 500 m thickness) compared to the other lithological units in succession, suggesting rifting of the basin. At this unit (4100 m - 4600 m) the Mvule # 1 achieved the thermal gradient temperature ranging from 238° C - 267° C (1 km = 58° C, therefore 4.1km = 50X4.1 and 4.6km = 58X4.6). These temperatures are over estimated and do not match with the one calibrated in the burial model using measured vitrinite reflectance values (200° C). However, the Shale Unit is a good source rock of the entire studied section, showing organic richness between 2.2-3.4% TOC and maturity levels between 1.2-1.5% Rv (4100m - 4600 m).

Conclusion

The investigation of the Mvule # 1 well provides the following insight on the organic richness, kerogen type, hydrocarbon generation, deposition environments and age of the studies section:

- The organic richness showed the highest TOC values of the entire well are encountered in the Shale Unit, varying from 2.2% to 3.4% suggesting a good source rock of the entire section.
- Four palynofacies zones have been recorded from this study (labelled 1-4), characterised by both terrestrial and marine derivatives. The assessment of depositional environments show marginal dysoxic-anoxic shelf, proximal suboxic-anoxc shelf and more oxic distal shelf setting conditions.
- The overall studied samples from Mvule #1 well are dominated by high abundances of dinoflagellate cysts (palynomorphs - kerogen Type II), phytoclasts (i.e., degraded brown wood and cuticle - kerogen Type III and black wood - kerogen Type IV) and AOM (kerogen Type I), with low abundance of sporomorphs throughout the succession. Therefore, the entire well being represented by kerogen Type II and III, a good oil and gas prone kerogen (Dow 1977, Tissot and Welte 1978, Peter and Cassa 1994). It is probable that the Mvule facies were source rocks for wet and dry gas with possibility of light oil generation as shown in maturity data.
- The present study, currently propose three assemblage bioevents (labelled 1-3) common from the late Albian-late Cretaceous section in the Tanzanian Offshore Basin; *Litosphaeridium siphoniphorum* Event (Late Cenomanian); *Adnatosphaeridium tutulosum* and

Hapocysta peridctya Event (Intra late Cenomanian-Late Albian Event); and *Palaeohystrichophora infusorioides* (Late Albian).

- Burial modelling indicates that the Shale Unit entered the oil window in the late Miocene (~10 Ma) and is continuing to produce hydrocarbons at present day.
- The high temperature in the Shale Unit (4100 m - 4600 m) during the burial diagenesis (238° C - 267° C) has probable the resulted in the loss of up to 50% of the organic carbon content (Raiswell and Berner 1987). Therefore, the TOC content of the Shale Unit could have been at least twice of 3.4% today.

Acknowledgements: We would like to thank the Tanzania Petroleum Development Corporation for fund support, samples materials and permission to publish this work. We are grateful to acknowledge Martin Pearce from Applied Evolution Biostratigraphic Consultants for providing his valuable expertise in Cretaceous species and bioevents, which significantly improved the manuscript biostratigraphy.

REFERENCES

Archangelsky, S., Barreda, V., Passalia, M.G., Gandolfo, M., Pramparo, M., Romerp, E., Cúneo, R., Zamuner, A., Iglesias, A., Lloewns, M. and Puebla, G.G. 2009. Early angiosperm diversification: evidence from southern South America. *Cretaceous Research*, 30 (5), 1073-1082.

Atta-Peters, D. 2013. Occurrences of elaterate pollen from the Lower Cretaceous of Ghana: Implications for biostratigraphy and palaeoclimatology. *International Letters of Natural Sciences,* 4: 54-66

Atta-Peters, D and Achaegakwo, C. A. 2016. Palynofacies and palaeoenvironmental significance of the Albian-Cenomanian succession of the Epunsa-1 well, onshore Tano Basin, western Ghana. *Journal of African Earth Sciences,* 114: 1-12.

Barker, C. A and Pawlewicz, M. J. 1994. Calculation of vitrinite reflectance from thermal histories and peak temperatures. A comparison of methods. In: MUKHOPADHYAY, P. K. and DOW, W. G. (eds.) Vitrinite reflectance as a maturity parameter. Applications and limitations. *American Chemical Society, Symposium series* 570 (14), 216-229.

Bergen, P. F., Janssen, N. M. M., Alferink, M. and Kerp, J. 1990. Recognition of organic matter types in standard palynological slides. *Mededelingen Rijks Geologische Dienst*, 45: 9-13.

Cavalli-Sforza, L. L. and Edwards, A. W. F. 1967. Phylogenetic Analysis –Models and Estimation Procedures. *The American Journal of Human Genetics,* 19: 233-257.

Cole. J. M., Abdelrahim, O. B., Hunter, A. W., Schrank, E., and Suhaili Bin Ismail, M. 2017. Late Cretaceous spore-pollen zonation of Central African Rift System (CARS), Kaiking Trough, Muglad Basin, South Sudan: angiosperm spread and links to the Elaterates Province. *Palynology,* 41: 547-578.

Deaf, A. S. 2009. Palynology, palynofacies and hydrocarbon potential of the Cretaceous rocks from northern Egypt. University of Southampton. *(Published PhD thesis, available online at https//www.eprints.soton.ac.uk/168943).* 348.

Deaf, A. S., Harding, I. C., and Marshall, J. E. A. 2014. Cretaceous (Albian? Early Santonian) palynology and stratigraphy of the Abu Tunis 1x borehole, northern Western Desert, Egypt. *Palynology*. 38: 51-77.

Dodsworth, P. 2004. The distribution of dinoflagellate cysts across a Late Cenomanian carbon isotope ($\delta^{13}C$) anomaly in the Pulawi borehole, central Poland. *Journal of Micropalaeontology*. 23: 77-80.

Eisawi, A., Awad B. Ibrahim, Omer Babiker A. Rahim and Eckart Schrank, 2012. Palynozonation of the Cretaceous to Lower Paleogene strata of the Muglad Basin, Sudan, Palynology, 36: 2, 191-207,

Helby, R., Morgan, R., and Partridge, A. D. 1987. A palynological zonation of the Australian Mesozoic. In: P. A. Jell (Ed.). Studies in Australian Mesozoic palynology. *Memoir of the Association of Australasian Palaeontologists,* 4: 1-94.

Herngreen, G. W. F., Kedves, M., Rovnina, L. V., and Smirnova, S. B. 1996. Chapter 29C. Cretaceous palynofloral provinces: a review. In: Jansonius, J., McGregor, D. C. (Editors). Palynology: Principal and Applications. *American Association of Stratigraphic Palynologists Foundation.* 3: 1157-1188.

Hillier, S. and Marshall, J.E.A. 1992. Organic maturation, thermal history and hydrocarbon generation in the Orcadian Basin, Scotland. *Journal of the Geological Society, London,* 149: 491-502.

Jarvie, D. M., 1991. Total organic carbon (TOC) analysis: Chapter 11: geochemical methods and exploration, 113-118.

Kagya, M. 1996. Geochemical characterization of Triassic petroleum source rocks in the Mandawa Basin,Tanzania. *Journal of African Earth Sciences*, 23: (1), 73-88.

Kajato, H. 1989. Evolution of Sedimentary Basins in Tanzania. Tanzania Petroleum Development Corporation, *Empresa Nacionale de Hidrocarbonetos Archives*, Maputo.

Kapilima, S. 2003. Tectonic and evolution of sedimentary coastal basin of Tanzania during the Mesozoic times. *Tanzania Journal of Science.* 29: 1-16.

Kaska, H.V. 1989. A spore and pollen zonation of the Early Cretaceous to Tertiary non-marine sediments of Central Sudan: *Palynology.* 131, 79-90.

Kent, P. E., Hunt, J. A., and Johnson, D. W. 1971. The geology and geophysics of coastal Tanzania. *Institute of Geological Sciences and Geophysics.* 6: 1-101.

Mayagilo, J. F. 1989. An Investigation of the Palynology of the Upper Jurassic to Lower Cretaceous strata from Songo Songo 5 well Offshore, South East Tanzania. Ph. D Thesis (Unpublished), University of Sheffield. 1-143.

Mbede, E. I. 1991. The sedimentary basins of Tanzania – a reviewed: *Journal of African Earth Sciences.* 13: 291-297.

Mpanju, F. and Philp, R. P. 1994. Organic geochemical characterisation of bitumens, seeps, rock extracts and condensates from Tanzania. *Organic Geochemistry,* 21: (3-4), 359-371.

Msaky, E. S. 1995. Palynological biostratigraphy of Cretaceous sediments, Rufiji Basin, Tanzania. *Tanzania Journal of Science*. DSM. 21: 85-108.

Msaky, E. S. 2011. Middle Jurassic to Earliest Late Cretaceous palynoflora, coastal Tanzania. *Palaeontographica, Abt. B, Palaeobotany-Palaeophytology.* 286: (1-3), 99.

Mukhopadhyay, P. K. and Dow, W. G. (eds.) 1994. Vitrinite reflectance as a maturity parameter. Applications and limitations. *American Chemical Society*, Series 570, Washington. 294.

Pearce, A. M., Jarvis, I., and Tocher, B. A. 2009. The Cenomanian-Turonian boundary event, OAE2, and

palaeoenvironmental change in epicontinental seas: new insights from the dinocyst and geochemical records. *Palaeogeography, Palaeoclimatology, Palaeoecology*, 280: 207-234.

Schluter, T., and Hampton, C. 1997. Geology of East Africa. Borntraeger, Berlin, 484.

Schrank, E. and Awad, M. Z. 1990.: Palynological evidence for the age and depositional environment of the Cretaceous Omdurman Formation in the Khartoum area, Sudan. *Berliner Geowissenschaftliche. Abhandlungen Reihe.* A 120: 169-182.

Schrank, E. 1994. Palynology of the Yesomma Formation in the Northern Somalia: A study of pollen, spores and associated phytoplankton from the Late Cretaceous *Palmae* province. *Palaeontograhica Abhandlungen.* B 231: 63-112.

Schrank, E. and Mahmoud, M. S. 1998. Palynology (pollen, spores and dinoflagellates) and Cretaceous stratigraphy of the Dakhla Oasis, Central Egypt. *Journal of African Earth Sciences,* 26: 167-193.

Srivastava, V. 1994. A Middle Cretaceous microflora assemblage from coastal Tanzania. *Journal of Palynology*. 30: 35-44.

Srivastava, V. and Msaky, E. 1999. Albian-Cenomanian microfloral assemblages from coastal Tanzania. University of Dar es Salaam, *Palaeoecology of Africa and surrounding Island and Antarctica, Special Edition.* 26: 31-44.

Tissot, B. P. and Welte, D. H. 1978. Petroleum formation and occurrence. *Springer-Verlag*, New York, 538.

Raiswell, R. and Berner, R. 1987. Organic carbon losses during burial and thermal maturation of normal marine shales. *Geology*, 15 (9), 853-856.

Tanzania petroleum development corporation (TPDC) geological internal report, 1979. Evolution of sedimentary basins. *Tanzania Petroleum Development Corporation, Dar es Salaam,* Unpublished report, 1-10.

Tanzania petroleum development corporation (TPDC) geological internal report, 2005. Development of sedimentary basins of Tanzania. *Tanzania Petroleum Development Corporation, Dar es Salaam,* Unpublished report.

Torsvik, T. H., and Cocks, L. R. M. 2017. Earth history and Palaeogeography *Cambridge University Press*. 317.

Tyson, R. V. 1995. Sedimentary organic matter: organic facies and palynofacies. Chapman and Hall, London, 615.

Wood, G. D., Gabriel, A. M., and Lawson, J.C. 1996. Palynological techniques-processing and microscopy. In Jansonius, J., McGregor, D. C., (Eds), Palynology: Principal and Applications. *American Association of Stratigraphic Palynologists Foundation.* 1: 29-50.

****